Journal of Cleaner Production 261 (2020) 121184

Contents lists available at ScienceDirect

Journal of Cleaner Production

journal homepage: www.elsevier.com/locate/jclepro

Review

A review on PEM electrolyzer modelling: Guidelines for beginners

D.S. Falcão*, A.M.F.R. Pinto**

CEFT - Transport Phenomena Research Center, Chemical Engineering Department, Oporto University, Engineering Faculty, Rua Dr. Roberto Frias, 4200-465, Porto, Portugal

ARTICLE INFO

Article history:
Received 12 September 2019
Received in revised form
2 March 2020
Accepted 16 March 2020
Available online 18 March 2020

Handling Editor: Prof. Jiri Jaromir Klemeš

Keywords:
PEM Electrolyzer
Modelling
Review

ABSTRACT

From a sustainability perspective, a synergy between hydrogen, electricity and Renewable Energy Sources (RES) is particularly attractive. A combination of Proton Exchange Membrane (PEM) fuel cells and PEM electrolyzers provides a back-up system for RES avoiding the intermittency: electrolyzers convert the excess of energy from RES into hydrogen and PEM fuel cells use this hydrogen to convert it back into electricity when it is needed. Models are an essential tool in electrolyzer development because it allows to understand the influence of different parameters on the electrolyzer performance enabling an efficient simulation, design and optimization of electrolyzer systems. Modelling studies have been developed with different degrees of complexity. This review presents a compilation of published models focusing on the main equations used to predict cell voltage, including reversible voltage, activation losses, ohmic losses and mass transport losses. Special sections are devoted to dynamic behaviour, two-phase flow effects and inclusion of thermal effects in model development. Also, a brief description of empirical/semi-empirical models is provided. This review aims to provide the main guidelines for the beginners on PEM electrolyzer modelling and, for this purpose, includes a section with the technology basic principles.

Contents

1. Introduction

Among various alternatives to produce hydrogen, the

* Corresponding author.
** Corresponding author.
E-mail addresses: dfalcao@fe.up.pt (D.S. Falcão), apinto@fe.up.pt (A.M.F.R. Pinto).

https://doi.org/10.1016/j.jclepro.2020.121184
0959-6526/

Nomenclature

Symbol (Unit)	Meaning
C(mol/cm^3)	Concentration of reactants/products
C_0 (mol/cm^3)	Reference concentration
E_{act} (J/mol)	Activation energy
E_{cell} (V)	Open circuit voltage
E^0_{th}	(V) Thermoneutral voltage at standard state
E^0_{rev}	(V) Reversible cell potential
F (C/mol)	Faraday constant
H(J/mol)	Enthalpy
I (A)	Current
i (A/cm^2)	Current density
i_{lim} (A/cm^2)	Limit current density
$i_{0,a}$(A/cm^2)	Anode exchange current density
$i_{0,c}$ (A/cm^2)	Cathode exchange current density
$i_{0,ref}$ (A/cm^2)	Exchange current density at reference temperature
n	Number of electrons transferred in the reaction
Nc	Number of electrolyzer cells
P	(Pa) Partial pressure of reactants/products
P_0 (Pa)	Standard pressure
Q (C)	Charge
R (J/molK)	Ideal gas constant
R_{cell} (Ω)	Electrolyzer cell resistance
T	(K) Electrolyzer temperature
T_a (K)	Anode temperature
T_c (K)	Cathode temperature
T_{ref} (K)	Reference temperature
V (V)	Electrolyzer voltage
$V_{Act,a}$ (V)	Anode activation overpotential
$V_{Act,c}$ (V)	Cathode activation overpotential
V_{Diff} (V)	Diffusion or concentration overpotential
z	Charge number

Greek symbols

α_a	Charge transfer coefficients at anode
α_c	Charge transfer coefficients at cathode
ΔG	(J/mol) Variation of Gibbs energy
ΔG^0_R	(J/mol) Gibbs free energy of reaction
ΔH^0_R	(J/mol) Enthaphy of reaction
k	Fraction of proton back-permeation to total proton permeation
λ	Membrane water content
δ	(cm) Material thickness
σ	(S/cm) Material conductivity

electrolysis using renewable energy is nowadays considered an option with potential to overcome the limitations of the intermittency occurring on typical renewable energy sources stations such as wind parks. Electrolyzers could convert the electricity provided from RES into chemical energy and combined with fuel cells could transform hydrogen back into electricity. This system should lead to an efficient storage and rapid wider diffusion of the electricity to the grid.

In particular, PEM electrolyzers have advantages when compared to the alkaline devices: they are less caustic, can be reversible devices and are able to operate at lower cell voltages, higher current densities, higher temperatures and pressures leading to higher efficiencies (80–90%). The main disadvantages are: high materials cost, cross permeation phenomena that increase with pressure and the presence of water vapor together with the produced hydrogen, requiring dehumidification (Carmo et al., 2013). While new materials are developed to reduce the total cost of the electrolyzer to enable the rapid commercialization, there is a need for further understanding of the main heat, mass and electrochemical processes, providing realistic predictions. Mathematical models play, at this point, an important role facilitating the dynamic connection between the electrolysis system and an intermittent electrical source.

In literature, models with different degrees of complexity can be found. Analytical models are a satisfactory tool to recognize the effect of the main variables on electrolyzer performance recurring to simplified considerations to simulate a fairly accurate polarization curve. Empirical/semi-empirical models allow the prediction of the electrolyzer behavior as a function of operating conditions (such as pressure, temperature) recurring to simple empirical equations. The main disadvantage is that, generally, the application of this kind of models is restricted to the range of operating conditions studied and for that specific electrolyzer design. Mechanistic models use differential and algebraic equations which are derived considering the electro-chemistry phenomena that occur in the electrolyzer and are numerically solved by different methods. These models involving extensive calculations accurately predict the polarization curve and the flux and concentration of multiple species in the electrolyzer, conducing however to simulation times considered too high for real time applications.

Regarding PEM electrolyzer modeling state of the art, the number of publications is considerably lower when compared to the number of papers on fuel cell modeling. The earliest models for PEM electrolyzers were reported in 2002 (Onda et al., 2002). Since then, some works, including those taking into account the cell dynamic behavior, were reported (Nie et al., 2009; Nie and Chen, 2010; Awasthi et al., 2011; García-Valverde et al., 2012). Review papers considering models to simulate eletrolyzers performance and/or specific phenomena occurring in a particular electrolyzer component are very useful to the research community, not only by providing an easier state-of-the art perception but also by offering a range of input parameters and guidelines useful in the development of new models. In the last few years, some reviews were published: a review focused on PEM water electrolysis including a section on modeling PEM water electrolysis (Carmo et al., 2013) and a recent one (Olivier et al., 2017) presenting a very complete review for low-temperature electrolysis system modeling (including alkaline and PEM technologies) with a classification of the models analyzed based on different criteria such as the physical domains involved or the modeling approaches. These review papers are, obviously, of extreme importance to the research community but they lack a more comprehensive description of the theory behind the PEM electrolyzers' operation principle. The main goal of the present review is to be a starting point to those interested in the PEM electrolyzer modeling area, providing a simple compilation of the models published in the last years, including the equations used to model cell voltage and enlightening important aspects that should be taken into account on the development of PEM electrolyzer models, as well as the basic principles of electrolyzer operation. A summary of the equations used to calculate the electrolyzer voltage is presented, plus the software used to implement the models. Because of its importance, special sections devoted to thermal effect, dynamic behavior inclusion and two-phase flow effects, in some models, are considered. A brief description of empirical/semi-empirical models is also provided.

2. Basic principles

As seen in Fig. 1, a PEM electrolyzer is an electrochemical energy converter which uses electricity to oxidize water, producing oxygen and protons in the anode side. As oxygen is produced, it leaves the device while the protons pass through the membrane and electrons circulate via an external circuit. At the cathode side, the electrons reduce the protons, producing hydrogen. In a PEM FC the reverse happens, with hydrogen and oxygen producing a DC electric current, water and heat. The basic design of an electrolyzer consists of two half cells with a thin, proton conducting and electron insulating PEM at the center of the cell. Going outwards from each side of the membrane, there is a porous catalyst layer on each side of the membrane, where the reactions occur. The PEM and the double catalyst layer form the Membrane Electrode Assembly (MEA). Enveloping the MEA, there is the current collector that physically and electrically connects the catalyst layer to the bipolar plate. Even so, the bipolar plate is the structure that provides physical integrity to the cell, provide pathways for products and reactants and separate one cell from the other in a stack.

The reactions occurring in a PEM electrolyzer (anodic, cathodic and global) are presented below:

Anodic reaction: $H_2O \rightarrow 2H^+ + \frac{1}{2}O_2 + 2e^-$ (1)

Cathodic reaction: $2H^+ + 2e^- \rightarrow H_2$ (2)

Global reaction: $H_2O \rightarrow H_2 + \frac{1}{2}O_2$ (3)

Equations (1) and (2) are generally known as Oxygen Evolution Reaction (OER) and Hydrogen Evolution Reaction (HER), respectively. equation (3) is the global reaction resulting from the sum of the two electrochemical half reactions which take place at the electrodes under acidic media and need an electrical DC power source to occur. An electrical DC power source is connected to the electrodes and the decomposition of water starts when a DC voltage higher than thermodynamic reversible potential is applied. The water can be supplied to the anode or cathode side, the majority of PEM electrolyzers operate with a water anode feed because water is consumed at this side. Under reversible conditions (without losses), the potential difference between the anode and cathode electrodes is called the reversible cell potential E^0_{rev}, corresponding to the minimal electrical work that is needed to split up water if the necessary contribution of thermal energy is present. At standard state (P = 1 atm and T = 298.15 K) the Gibbs free energy of the global reaction (3) is 236.483 kJ/mol (this positive value indicates that the water split reaction is a nonspontaneous process, requiring energy from an external source). Knowing the values of Gibbs free energy of reaction (ΔG^0_R), the Faraday constant (F) and the number of moles of electrons transferred during the reaction (n) enables the estimation of E^0_{rev} (Bessarabov, wang et al., 2015):

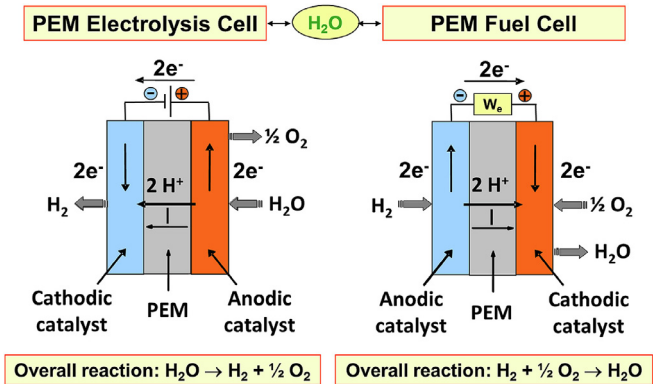

Fig. 1. Schematic representation of PEM EL and PEM FC (Lamy, 2016).

$$E^0_{rev} = \frac{\Delta G^0_R}{nF} = 1.229\ V \quad (4)$$

Considering that no external heat source is available, the entire energy needed for the reaction occur (ΔH^0_R) must be delivered by means of electrical energy. In the case of the water split reaction (3), the value for ΔH^0_R under standard conditions is −285.83 kJ/mol. Therefore, the voltage required to occur the referred reaction is higher than the E^0_{rev} and known as thermoneutral voltage at standard state (E^0_{th}) (Bessarabov, wang et al., 2015):

$$E^0_{th} = \frac{\Delta H^0_R}{nF} = 1.481\ V \quad (5)$$

Once the current passes through the cell, the actual voltage for the water splitting reaction becomes higher that the reversible cell potential due to irreversible losses occurring in the cell. These losses can be split into Faradaic (activation losses) and non-Faradaic losses (ohmic and mass transfer or concentration losses). Activation losses are due to electrochemical reaction activation: there is a shift from thermodynamic equilibrium which reduces the velocity of the reactions taking place at the anode and cathode electrodes surface (Bessarabov, wang et al., 2015). Some of the available cell thermodynamic potential must be lost because the charge build-up is changed with a noticeable impact on the activation barriers. The activation losses (V_{act}) are the major cause contributing to lower efficiency when operating a cell at high voltage and low current density values and are governed by Faraday's law, that state that the amount of a gas produced by an electrochemical process can be related to the electrical charge consumed by the cell:

$$Q = nzF \quad (6)$$

where **Q is** the charge in Coulombs (C) and z is the charge number.

Considering equation (6) and Arrhenius equation, it is possible to deduce Butler-Volmer equation, which is commonly used to describe activation overpotential, as referred in section 3.1.2. All the considerations and equation developments are very well explained and can be found in Bessarabov et al. (2015).

In the middle of the operating range the predominant losses are due to the electrolyzer cell resistance (R_{cell}) generated by the ionic and electronic conduction. The total ohmic losses are determined by the application of Ohm's law, as referred in section 3.1.4. Usually, due to the high conductivity of commonly used materials (as titanium), it is often considered that electron transport is much faster than protonic transport and, therefore, only ohmic losses due to proton transport through the PEM are taken into account.

At very high current densities, the major losses (the concentration losses or diffusion overpotential, V_{diff}) are due to mass transport limitations and are not considered by many authors since electrolyzers usually do not operate at high current densities. However, some works (Hwang et al., 2009; Lebbal and Lecœuche, 2009; Marangio et al., 2009; Kim et al., 2013) considered these losses. At high current densities (higher than 2 A/cm^2) the gas bubbles produced can block the active area, damage the contact between the electrode and the electrolyte and decrease the catalyst utilization. The mass transport losses are governed by Nernst equation stating that the overpotential due to mass transport limitation increases with the increase in the product species

concentration at the reaction interface (Bessarabov, wang et al., 2015), as referred in section 3.1.3. Fig. 2 depicts an example of a PEM electrolyzer polarization curve with the contribution of the three losses referred above: activation, ohmic and mass transport losses.

3. Models review

3.1. Voltage

The most common representation of the electrolyzer performance is the polarization curve that represents the relation between the current density and the voltage.

Nafeh (2011) modeled the electrolyzer voltage (V) using the following expression:

$$V = N_c\left(E_{Cell} + V_{Act,c} + V_{Act,\,a} + iR_{cell}\right) \tag{7}$$

where *Nc* is the number of electrolyzer cells, E_{cell} is the open circuit voltage $V_{Act,a}$ and $V_{Act,c}$ are the anode and cathode activation overpotentials, i is the current density and R_{cell} is the electrolyzer cell resistance (ohmic losses). Similar expressions are used by almost all the authors (Harrison et al., 2005; Görgün, 2006; Brown et al., 2008; Ni et al., 2008; Awasthi et al., 2011; García-Valverde et al., 2012; Myles et al., 2012; Aouali et al., 2014; Chandesris et al., 2015). This expression excludes the mass transport losses since, as referred before, electrolyzers usually do not operate at high current densities.

An empirical equation to determine the electrolyzer cell voltage is presented by Atlam and Kolhe (2011) and another is used by Sossan et al., 2014:

$$V = 0.326I + 1.476 \tag{8}$$

and

$$V = 33.1 - 43.0 \times 10^{-3} I \tag{9}$$

Where I is the electrolyzer current.

Considering the expressions used for the electrolyzer voltage calculation, it seems that almost all the authors used the same expression, varying only the importance given to the losses occurring in the electrolyzer with most of the authors neglecting the concentration losses. Some empirical expressions can be found and should be applied carefully because they are developed for a specific electrolyzer design and a particular range of operating conditions.

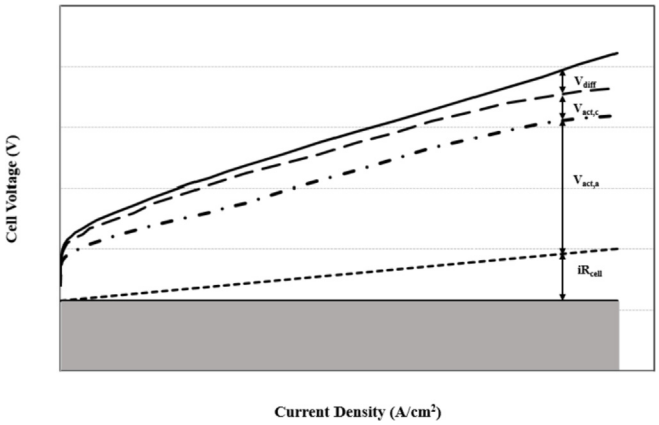

Fig. 2. Typical PEM electrolyzer polarization curve with the contribution of activation and ohmic and mass transport losses.

3.1.1. Open circuit voltage

The open circuit voltage is usually determined using the Nernst equation. This equation, or very similar ones, is used in many works reported in literature (Han et al., 2016; Yigit and Selamet, 2016; Ruuskanen et al., 2017; Moradi Nafchi et al., 2019; Toghyani et al., 2019):

$$E_{cell} = E^0_{rev} + \frac{RT}{2F}\left[\ln\left(\frac{P_{H_2} p_{o_2}^{1/2}}{P_{H_2}0}\right)\right], \tag{10}$$

where P is the partial pressure of reactants/products, T is the temperature, F is the Faraday constant and E^0_{rev} is the reversible cell potential at standard temperature and pressure. It is calculated by equation (4), as referred in section 2, and is used by several authors (Görgün, 2006; Brown et al., 2008; Aouali et al. 2014, 2017; Abdol Rahim, Tijani et al., 2015; Saeed and Warkozek, 2015; Mohamed et al., 2016; Yigit and Selamet, 2016). Some authors considered empirical temperature dependent expressions (Dale et al., 2008; Awasthi et al., 2011; Abdin et al., 2015; Han et al., 2016; Ruuskanen et al., 2017; Moradi Nafchi et al., 2019):

$$\mathbf{E^0_{rev}} = 1.5241 - 1.2261 \times 10^{-3}T + 1.1858 \times 10^{-5}Tln(T) + 5.6692 \times 10^{-7}T^2 \tag{11}$$

$$\mathbf{E^0_{rev}} = 1.229 - 0.9 \times 10^{-3}(T - 298) \tag{12}$$

$$\mathbf{E^0_{rev}} = 1.229 - 0.9 \times 10^{-3}(T - 298) + 2.3\frac{RT}{4F}Log\left(P^2_{H_2}P_{O_2}\right) \tag{13}$$

In Garcia-Valverde, Espinosa et al (2012) the open circuit potential is determined by an empirical equation for atmospheric pressure condition, depending from temperature, expression also in others work (Agbli et al., 2011; Kaya and Demir, 2017):

$$E_{cell} = 1.5184 - 1.5421 \times 10^{-3}T + 9.523 \times 10^{-5}Tln(T) + 9.84 \times 10^{-8}T^2 \tag{14}$$

Kim et al. (2013) introduced a new parameter, k, in E_{cell} calculation, as follows:

$$E_{cell} = -(1-k)\frac{\Delta G}{2F} \tag{15}$$

where ΔG is the Gibbs energy variation and k the fraction of proton back-permeation relative to total proton permeation. The term 1-k is included to take into account the effect of hydrogen permeation and proton back-permeation.

Since non-standard pressure and temperature conditions are generally used, other equations must be applied (more details can be found in Marangio et al. (2009)). The equations reported in this work enable the consideration of different temperatures at the anode and cathode sides, leading to more accurate values of E^0_{rev}.

Some equations are available to use for open circuit voltage and reversible potential calculations. If the electrolyzer works at standard temperature and pressure, simpler equations could be used with no significant errors associated. However, for different temperatures and higher pressures the use of more accurate equations is recommended.

3.1.2. Activation overpotential

Activation losses occur, as referred, because of the necessity to sacrifice some potential to activate the electrochemical reactions

taking place at anode and cathode sides, as described in Section 2.

One of the more common expressions for activation overpotential calculations is based in the Butler-Volmer equation and is used by many authors (Marangio et al., 2009; Agbli et al., 2011; Awasthi et al., 2011; Kim et al., 2013; Abdin et al., 2015; Yigit and Selamet, 2016; Ruuskanen et al., 2017; Sartory et al., 2017; Moradi Nafchi et al., 2019) on electrolyzer model development:

$$V_{Act} = \frac{RT_a}{\alpha_a F} arcsinh\left(\frac{i}{2i_{0,a}}\right) + \frac{RT_c}{\alpha_c F} arcsinh\left(\frac{i}{2i_{0,c}}\right) \quad (16)$$

where $i_{0,a}$ and $i_{0,c}$ are the exchange current density at anode and cathode, respectively and α_a and α_c are the charge transfer coefficients at anode and cathode, respectively.

Some authors (Choi et al., 2004; Harrison et al., 2005; Biaku et al., 2008; Dale et al., 2008; Ni et al., 2008; Aouali et al. 2014, 2017; Aouali et al. 2017) used a similar expression but with a factor of 2 coupled to the charge transfer coefficient, as follows:

$$V_{Act} = \frac{RT_a}{2\alpha_a F} arcsinh\left(\frac{i}{2i_{0,a}}\right) + \frac{RT_c}{2\alpha_c F} arcsinh\left(\frac{i}{2i_{0,c}}\right) \quad (17)$$

Other authors used a simplified expression (Görgün, 2006; Lebbal and Lecœuche, 2009; Nafeh, 2011; Abdol Rahim et al., 2015; Saeed and Warkozek, 2015):

$$V_{Act} = \frac{RT}{n\alpha F} ln\left(\frac{i}{i_0}\right) \quad (18)$$

This equation can be applied for both sides, anode and cathode (García-Valverde et al., 2012). The values reported in literature for the exchange current density coefficients are very dissimilar. For this reason, some authors decided to choose the values that better adjust their models. These values increase with temperature, therefore, an expression relating it with the temperature is very useful and is presented by Garcia-Valverde, Espinosa et al. (2012) applying an Arrhenius expression, as follows:

$$i_0 = i_{0,ref} exp\left[-\frac{E_{act}}{R}\left(\frac{1}{T} - \frac{1}{T_{ref}}\right)\right] \quad (19)$$

where E_{act} is the activation energy of the electrode and $i_{0,ref}$ is the exchange current density measured at a reference temperature T_{ref}.

Regarding the charge transfer coefficient (CTC), the most part of the authors consider it constant with temperature, however, some works presented an estimation of the CTC depending on the operating temperature. Biaku et al. (2008) reported that there is a reasonable variation of the anode CTC from the called symmetry factor (0.5 – the most common value used in the literature). The authors noticed that the average anode CTC changes from 0.18 to 0.42 within a temperature range of 20–60 °C. Tijani et al. (2018) simulated the CTC values (but the model was successfully validate with experimental data). The simulation results show that as the electrolyzer operating temperature increases (range 10–90 °C), the values of CTC also increase but this increment is more pronounced at the anode (ranges between 0.807 and 1.035) compared to cathode (ranges between 0.202 and 0.259) electrodes. The authors also observed that activation overvoltage decreases when the CTC increases from 0.1 to 2.0 both at anode and cathode electrodes. Curiously the pressure doesn't seem to affect CCT values, remaining the same even at balanced and unbalanced pressure. Touré et al. (2018) estimated CTC first from the current-voltage characteristic of a fuel cell, by using only the activation polarization and found a value of 0.669. Then the Lagrange's undetermined multiplier technique was used to evaluate the transfer coefficient and was found a value of 0.222. The authors believe that the Lagrange's multiplier technique (that takes into account the ohmic polarization, the activation polarization and also the current-power characteristic of the device) can be a better way to estimate of the charge transfer coefficient.

Table 1 displays the values reported in the literature for exchange current density for anode and cathode reactions and also for the charge transfer coefficients for both sides.

To describe the activation losses, almost all the authors used an expression based on Butler-Volmer equation. However, the formulation of this equation is not consensual; some authors used a factor of 2 coupled to the charge transfer coefficient. The values for the charge transfer coefficient must be carefully chosen taking into account this consideration. The values reported for exchange current density are very different; the values are generally higher for the cathode side, indicating that the reaction kinetics is faster than for the anode side. The most common value chosen for charge transfer coefficients is 0.5. Some authors consider this coefficient temperature dependent.

3.1.3. Mass transport overpotential

The mass transport losses occur when the current density is high enough to impede the access of reactants to active sites by the overpopulation of reacting molecules and for this reason slowing down the reaction rate (Biaku et al., 2008). In PEM electrolyzer, usually, this behavior is not observed until moderate operating current densities (1.6 A/cm^2). Accordingly, the current should be limited in order to reach high efficiencies (Barbir, 2005).

The mass transport overpotential (also usually called as diffusion overpotential – V_{Diff}) can be estimated using the Nernst equation as reported in Marangio et al. (2009):

$$V_{Diff} = \frac{RT}{nF} ln\frac{C}{C_0} \quad (20)$$

where C is the concentration of oxygen or hydrogen at the interface membrane-electrode and C_0 is a working concentration taken as the reference concentration. This equation can be applied for both anode and cathode sides (Agbli et al., 2011; Kim et al., 2013; Abdin et al., 2015; Han et al., 2016; Aouali et al., 2017; Moradi Nafchi et al., 2019; Toghyani et al., 2019).

Saeed and Warkozek (2015) used an expression based on i_{lim}, the maximum current density that can be provided to the electrolyzer, so it reveals the maximum production rate permitted by the electrolyzer:

$$V_{Diff} = -\frac{RT}{nF} ln\left(1 - \frac{i}{i_{lim}}\right) \quad (21)$$

Mohamed et al. (2016) used a very similar expression but with a multiplicative factor on denominator, a, defined as the transfer coefficient of diffusion layer.

The mass transport losses are not relevant until moderate operating current densities. Under current densities of 1.6 A/cm^2, these losses can be neglected with no significant errors associated to voltage prediction.

3.1.4. Ohmic losses

The ohmic overpotential is related with the materials resistance to the protons flux. The magnitude of ohmic losses depends on the materials properties. Manufacturing techniques and processes are a significant aspect to reduce this overpotential (Biaku et al., 2008).

The standard Ohm's law is applied in all the works analyzed (Choi et al., 2004; Harrison et al., 2005; Biaku et al., 2008; Brown et al., 2008; Dale et al., 2008; Ni et al., 2008; Lebbal and

Table 1
Values reported in the literature for exchange current density and charge transfer coefficients for anode and cathode reactions.

Reference	$i_{0,a}$(A/cm^2)	$i_{0,c}$(A/cm^2)	α_a	α_c
Hwang et al. (2009)	0.5×10^{-3}	0.4×10^{-6}	0.5	0.25
Dale et al. (2008)	2.93×10^{-5}[a]	0.21[a]	n.r.	0.5
Kim et al. (2013)	10^{-2}	10^{-4}	n.r.	n.r.
Marangio et al. (2009)	10^{-13} to 10^{-6} [b]	10^{-13} to $10^{-6b)}$	2	0.5
Ni et al. (2008)	1.0×10^{-9}	1.0×10^{-3}	0.5	0.5
Harrison et al. (2005)	1.0×10^{-8}	9.0×10^{-2}	0.5	0.5
Choi et al. (2004)	1.0×10^{-7}	1.0×10^{-3}	0.5	0.5
Yigit and Selamet (2016)	2.0×10^{-7}	2.0×10^{-3}	2	0.5
Abdin et al. (2015)	1.0×10^{-7}	1.0×10^{-1}	0.8	0.25
Han et al. (2016)	0.5×10^{-6}	0.1	–	–
Biaku et al. (2008)	1.9×10^{-3}[a]	0.303[a]	0.257 [a]	0.5
Agbli et al. (2011)	1.548×10^{-3}	3.539×10^{-2}	0.7178	0.6935
Tijani et al. (2018)	1.0×10^{-9}	1.0×10^{-3}	0.864[c]	0.216[c]
Abdol Rahim, Tijani et al. (2015)	1.0×10^{-9}	1.0×10^{-3}	–	–
Toghyani et al. (2019)	10^{-6} to 10^{-1}	0.01–10	–	–
Lebbal and Lecœuche (2009)	0.13×10^{-3} [d]		0.452 [d]	
Brown et al. (2008)	0.01×10^{-4} [e]		0.5 [e]	

[a] Values for T = 25 °C extracted from adjust experimental data.
[b] Values chosen between this range that better fits the experimental results.
[c] Values for T = 30 °C.
[d] The authors determined a global value for I_0 and α by applying the non-linear least square method on real data given by the PEM electrolyser cell. The authors didn't report the units for I_0.
[e] The authors used a global value for I_0 and α.

Lecœuche, 2009; Agbli et al., 2011; Awasthi et al., 2011; Nafeh, 2011; Kim et al., 2013; Aouali et al., 2014; Abdin et al., 2015; Abdol Rahim et al., 2015; Saeed and Warkozek, 2015; Yigit and Selamet, 2016; Ruuskanen et al., 2017):

$$V_{Ohm} = RI = \frac{\delta}{\sigma} I \tag{22}$$

where δ is the material thickness and σ the material conductivity. This equation is usually applied to the membrane but can also be applied to diffusion and catalytic layers. Sartory et al. (2017), in their semi-empirical high pressure PEM water electrolyzer model, added a multiplier term (a(T,P)) to conductivity to enable the membrane conductivity calculation at different pressures and temperatures. More details are given in the referred work.

The membrane conductivity, considering Nafion, can be expressed as (Görgün, 2006; Lebbal and Lecœuche, 2009; Awasthi et al., 2011; Abdin et al., 2015; Abdol Rahim et al., 2015; Saeed and Warkozek, 2015; Yigit and Selamet, 2016):

$$\sigma = (0.005139\lambda - 0.00326) exp\left[1268\left(\frac{1}{303} - \frac{1}{\mathbf{T}}\right)\right] \tag{23}$$

where T is the electrolyzer temperature and λ is the membrane water content.

There is a consensus in the use of Ohm's law to describe the ohmic losses. This equation is commonly used to take into account the membrane resistance (which is the most significant) as well as the diffusion and catalytic layers' resistances.

3.2. Dynamic behaviour

The connection of the PEM electrolyzer to renewable intermittent and variable power sources is of crucial importance and, therefore, the consideration of dynamic behavior in the models has special interest. This inclusion involves a significant increase in the model complexity with the need of resolution of systems of Ordinary Differential Equations (ODE) or even Partial Differential Equations (PDE) for system control analysis in the first case and for sizing, chemical and thermal process design and analysis in the latter (Olivier et al., 2017).

Kim et al. (2013) introduced the dynamic effects by considering unsteady mass and energy balance equations for the two electrolyzer channels and the MEA separately. A simplification was proposed by assuming that the water and gas flow simultaneously at the same speed. The non-ideal gas behavior of high-pressure hydrogen was represented by a compressibility factor. The dynamic responses were numerically studied for changes in the average current density and in inlet water flow rates. However the model was not validated with experimental data.

Lebbal and Lecœuche (2009) developed an electrolyzer model split into two parts: electrical and thermal. The electrical model was developed for steady state conditions. The thermal model includes the dynamic temperature behavior for current and voltage. The electrical and thermal model parameters were predicted using different techniques. For the thermal model, the parameters were identified using the properties of a first order linear model. The model was used to develop monitoring algorithms. In particular, the monitoring of the temperature sensor allowed avoiding membrane hot point and tear providing an important tool to guarantee the electrolyzer safety control.

Garcia-Valverde, Espinosa et al. (2012) developed a semi-empirical model considering dynamic behavior in the H_2 production submodel and in the thermal submodel. The authors obtained the theoretical H_2 flowrate from the Faraday's law. The real H_2 flowrate at steady state was then computed incorporating the several losses and the dynamic response was estimated using a first order response system. The submodel parameters could be identified from a current-step response, measuring the time to reach the steady state in the hydrogen output. The thermal submodel also included the dynamic response for changes in temperature. Both the dynamic submodels were validated with experimental data and strengths and limitations of the modelling approach were presented.

The dynamic model of Görgün (2006) considered four ancillaries: anode, cathode, membrane and voltage. Each ancillary

dynamics and interaction between them was taken into account. Additionally, a storage ancillary was considered. The model was developed in Simulink. The results confirmed that the model can simulate correctly the transient behavior of the PEM electrolyzer. However, the model was not validated against experimental data. Awasthi et al. (2011) developed a similar model, with the same four blocks in Simulink. This model was validated with experimental results and reaching a good agreement. A similar approach was also followed by Yigit and Selamet (2016). The model was tested against dynamic changes and it responded with fast outputs. The loss of each system component at different current densities was considered in the numerical simulations. The results showed that the loss of the stack dominated the losses of other components in the region of high current densities due to the effect of the increasing pressure. The model was experimentally validated.

Agbli et al. (2011) used a model based in Energetic Macroscopic Representation (EMR) and described the dynamic evolution of the temperature in the stack and in the water tank. The thermal model parameters were obtained using experimental fitted values. Some of these parameters are specific of the experimental apparatus and experimental conditions reported by the authors. The model was also implemented in Simulink environment and experimental and simulated curves considering voltage responses and temperature evolutions showed good agreement against experimental data.

Oliveira et al. (2013) developed a physical multiscale and transient model for PEM electrolyzer anodes. This model presented results for a large set of operating parameters and material parameters in the anode modelling. The model development was based on an elementary kinetics approach alternative to the Butler-Volmer equation. The model results adjusted well both the in-house obtained experimental data and the published available experimental results.

Some examples of PEM electrolyzer models considering dynamic behavior are available; however, only a few are validated against experimental data. The model validation is an important issue to confer credibility to the developed models for the prediction of electrolyzer performance. Unlike what has been done for fuel cell systems, very few PEM electrolysis modelling works include input-output models which are suitable for diagnosis studies such as for example, degradation mechanisms.

3.3. Thermal effects

The consideration of thermal effects in the development of electrolyzer models is essential since it enables to describe the temperature distribution in the cell and its impact on efficiency and durability. Most of the available models are based on the analytical characterization of heat accumulation, production, exchange and transport terms together with the resolution of thermal balances. Some examples are here reported.

Lebbal and Lecœuche (2009) considered, in their model development, four major heat contributions: chemical reaction (entropy), chemical component thermodynamics (gases and water), external ambient temperature and Joule effect due to the current circulation. The thermal model produced the dynamic temperature impact for both current and voltage. The thermal model parameters were predicted using the properties of a first order linear model based on experimental measurements. As referred in Section 2.2, the model was used to develop monitoring algorithms.

The thermal submodel of Garcia-Valverde, Espinosa et al. (2012) based on the lumped thermal capacitance which is the overall thermal capacity of the electrolyzer. This important parameter was estimated from an experimental set of heating curves, thermally insulating the stack and turning off the auxiliary cooling system. A statistical comparison between experimental and simulated data concerning dynamic operating temperature calculation was done and good agreement was obtained. However, for other experiments some limitations were founded, namely, large errors were obtained for high current densities values.

Kim et al. (2013) included in their model the development the unsteady energy balance equations and obtained the temperature profiles after implementation and resolution. A linearly increasing distribution along the anode flow direction was found: the MEA was acting as heat source and the anode flow as the major heat carrier. A weakness of this model is the necessity of validation with experimental data.

Agbli et al. (2011) developed a thermal model with two degrees of freedom: the temperature along the electrolyzer and the water tank temperature. The thermal balance was established considering all heat sources and sinks (electrical energy released by overpotentials, heat flow evacuated from the environment and received by the water tank and the heat exchange between the device and the surrounding atmosphere). The model parameters were obtained using experimental values, literature values and water tank measures. The stack and tank predicted temperature evolutions showed notable agreement with the experimental data.

A similar approach was followed by Aouali et al. (2017), incorporating the thermal effect in the development of a model to simulate a PEM electrolyzer for hydrogen production. The thermal model included the heat exchange between the device and the surrounding atmosphere, the water reservoir thermal energy accumulation, the entropy flow of both heat sources and sinks and the heat losses by conduction. The model was successfully validated against experimental data from both the PEM electrolyzer stack and the water reservoir temperature profiles.

Toghyani et al. (2018) conducted a non-isothermal three-dimensional Computational Fluid Dynamics (CFD) numerical study to investigate the distribution of current density, temperature and pressure drop on an innovative spiral pattern anode and cathode flow fields. The model was able to provide precise data for mass and heat transfer, electrodes kinetics, and potential fields within the PEM electrolyzer. The model was validated against experimental data with a satisfactory agreement at low to medium currents densities. The model results showed that the spiral flow field conducted to a uniform distribution of produced hydrogen and current density and to a uniform distribution of temperature. However, non-uniformities were found at 90° bends due to stagnation of water and decrease in its velocity.

In spite of its importance, thermal effects are not included in the majority of the models available in literature, in particular those including the thermal architecture of the electrolysis system, fundamental to gain insight on the stack thermal behavior.

3.4. Empirical and semi-empirical models

Among the simpler approaches in electrolysis modelling the most common is the development of empirical and semi-empirical models. The first depends on parametric equations obtained by the mathematical handling of experimental data and generate parameters which do not have a physical meaning. The latter models are based on basic physical laws with physically meaningful parameters even though some or most of them are obtained from the use of empirical correlations. Some selected examples are next reported.

Atlam and Kolhe (2011) developed an electrical equivalent model for a PEM electrolyzer using the experimental results under steady-state conditions following the Faraday's Law. The model adjusts well the experimental results in the active region and produces an estimation of the hydrogen production rate, the power-hydrogen production rate and practical electrolyzer

efficiencies. This model is very useful to analyze the temperature and pressure effects on the electrolysis efficiency. The conductivity of the PEM electrolyzer cell is superior using higher temperatures and lower pressures. The pressure effects on the voltage are logarithmic. Although the model is empirical, it can be applied to different sizes of active area in addition to different parallel/series combinations of cells.

Santarelli et al. (2009) presented a useful method for the design of experiments that produces first-order regression models for the investigated dependent variables in terms of significant parameters. The results of the Yate's technique experimental design have been reported. Two analyses have been done at extreme stack operating conditions: 0.1 and 1 A/cm^2. This approach enables the establishment of analytical relations between the dependent variables (the stack voltage) and the explored independent variables (pressure, temperature, water flow and current). The authors concluded that pressure and temperature have a predominant effect on the electrolyzer performance while the voltage remains almost invariable with the water flow.

Biaku et al. (2008) developed a semi-empirical study regarding the temperature dependence of the anode charge transfer coefficient of a PEM electrolyzer stack. The charge transfer coefficient is a very significant model parameter to predict the current-voltage characteristics of electrolyzers providing insight into the properties of the electrode. The model results indicate that the anode charge transfer coefficient changes from 0.18 to 0.42 in the temperature range of 20–60 °C which is noticeably lower than the standard symmetry factor of 0.5.

Dale et al. (2008) used a semi-empirical equation to describe the performance of a 6 kW PEM electrolyzer stack. The authors considered the temperature dependence in reversible potential calculations. The experimental I–V curve obtained was predicted and nonlinear curve fitting algorithms were used to extract model critical parameters like anode and cathode exchange current densities and membrane conductivity.

As referred in Section 3.3, Lebbal and Lecœuche (2009) developed a thermal model producing the model parameters using the properties of a first order linear model based on experimental measurements.

Harrison et al. (2005) developed a semi-empirical equation to model the behavior of a 20-cell PEM electrolyzer stack. The model parameters, such as exchange current density and membrane conductivity were obtained from experimental data using a nonlinear curve fitting method.

Sartory et al. (2017) presented a semi-empirical zero-dimensional steady state model of an asymmetric high pressure PEM water electrolyzer where empirical parameters were established taking into account the experimental investigations on a 9.6 kW electrolyzer. The referred model is able to predict the stack voltage, gas production flow rates, water consumption and stack efficiency as function of input current, process temperature and production pressure. The results showed a satisfactory uniformity of measurements and simulations.

Becker and Karri (2010) developed predictive models for PEM electrolyzer system efficiency and hydrogen flow rate using neural network based Adaptive Neuro-Fuzzy Inference Systems. These models showed a very good agreement (accuracy of ± 3%) when compared with experimental data. The utilization of these models could be of special interest as generic virtual sensors for wide safety and monitoring applications.

Medina and Santarelli (2010) studied the water transport trough the membrane under different operating conditions. Based on experimental data obtained for the PEM electrolyzer, the Design of Experiments (DoE) methodology is used to obtain a regression model for the net electro-osmotic drag coefficient. The goal was to find the optimal operating conditions to reduce the amount of water driven from the anode side to the cathode side and, therefore, reduce the amount of water that has to be separated from the produced hydrogen.

There are several empirical/semi-empirical models available to simulate PEM electrolyzer performance. These models can be easily implemented to obtain polarization curves in real time calculations. However, a careful selection must be performed to pick-up those corresponding to the users' desired operating conditions and electrolyzer design.

3.5. Two-phase flow effects

In PEM electrolyzers, oxygen evolution at the anode and flooding due to water crossover at the cathode yield different two-phase transport conditions, which strongly affect performance. Unfortunately, there are only a few models which deal with these issues.

Arbabi et al. (2016) developed a 3D, two-phase flow model to investigate the oxygen bubble transportation through the GDLs of a PEM electrolyzer. The model used the Volume-of-Fluid (VOF) technique to simulate the gas-liquid interface through liquid-saturated porous media. The authors successfully validated their model with previous experimental microfluidic investigations. The model was used to calculate pressure variations in bubbles during propagation and the maximum threshold capillary pressure was suggested as a pointer of oxygen bubble removal effectiveness. The model can be used to help on designing and evaluating GDL microstructures for next generation electrolyzer materials.

Nie et al. (2008) presented a 3D CFD model considering two-phase flow (oxygen/water) effects in a basic anode bipolar flow-field of a PEM electrolysis cell aiming to examine flow characteristics in a bipolar plate and inside electrolyte cells. The authors used the mixture model to simulate the two phases solving the momentum and continuity equations for the mixture, the volume fraction equations for the secondary phase and algebraic expressions for the relative velocities. The model was only validated with the measurements of the pressure drop for single phase fluid dynamics, which represents a limitation of the referred work. The authors performed simulations with an oxygen bubble rate of 0–0.014 g/s and the results revealed that the average volume fraction of oxygen at the exit is higher when the mass flow rate of the oxygen bubbles increases.

Han et al. (2016) developed a two-phase transport model to study the liquid water distribution into the liquid/gas diffusion layer (LGDL) and an electrochemical performance model coupled with an equivalent resistance model. The model was successfully validated by comparison of predicted polarization curves with experimental results. However, the authors used the exchange current densities parameters values and membrane humidification degrees that better fit their experimental data. The effects of LGDL properties (contact angle, porosity and pore size) on the two-phase transport dynamics were studied and the liquid saturation distribution inside the LGDL was determined. Additionally, the influence of two-phase transport on the performance and efficiency of a PEM electrolyzer was examined. As main conclusions the authors reported that the liquid water saturation along the LGDL thickness direction is enhanced (with a consequent improving on cell performance) using higher porosities and/or pore size or using lower contact angles.

Lee et al. (2019) used pore network modelling to predict the saturations of oxygen gas and liquid water and the resultant permeability in sintered titanium powder-based porous transport layers (PTLs). The authors studied the influence of PTL-catalyst coated membrane (CCM) contact angle, pore and throat sizes and

porosity on two-phase flow transport under different operating conditions. As main conclusion, the authors strongly recommend the use of a backing layer, or a micro-porous layer, in order to enhance mass transport as well as interfacial contact.

Briguglio et al. (2013) developed a hydrodynamic study in an electrolyzer stack (with 10 cells). The study focuses on diffusional aspects concerning water mass distribution along the channels and was investigated using a CFD program. The model showed a reasonably uniform distribution of water along the channels and a homogeneous pressure inside the cells. A uniform water distribution in each cell allows avoiding gas accumulation inside the stack and hot spots formation that could damage the MEA. This type of analysis is very useful to identify operating conditions that conducts to a good water distribution in cells channels.

Myles et al. (2012) developed a species transport model within a high pressure oxygen-generating PEM water electrolyzer using the dusty-fluid model (DFM) when liquid water was fed to the cathode. Simulation results were validated with performance data obtained for Hamilton Sundstrand's high pressure oxygen generating assembly (HPOGA) at varying differential oxygen pressures. The dehydration of the cell was found to occur at a Damkohler number of 0.196. It was concluded that the electro-osmotic drag has a notable influence because of its direct and substantial effect on the necessary water flux for a given operating current density to avoid membrane dehydration.

3.6. Software used

The model equations usually need to be solved by using software stronger than Excel. Some authors do not provide any information on the software used. A compilation of the software's referred by some works to implement the developed models is presented in Table 2.

The software more extensively used to implement empirical models is Mathematica, while the majority of authors used Matlab to execute analytical/mechanistic models.

4. Conclusions

This review compiles the PEM electrolyzer models developed during the last years and presents the technology basic principles. Particular emphasis on the equations used to predict cell voltage, including open circuit voltage, activation losses, ohmic losses and mass transport losses is provided. Special sections are devoted to dynamic behavior, thermal effects and two-phase flow inclusion in model development. A brief description of empirical/semi-empirical models is also presented. Although the total number of articles published with PEM electrolyzer models is much lower than the total amount of papers devoted to PEM fuel cells models, in the last five years, interest in PEM electrolysis has increased and is expected to increase significantly in the next decade.

The models published are mainly empirical/semi-empirical and analytical models that can predict easily the PEM electrolyzer performance. Some of these models were not validated with experimental data, which is a handicap for its use to simulate PEM electrolyzer performance. Taking into account the main application of PEM electrolyzers (as a back-up system together with fuel cells to avoid RES intermittency) the dynamic behavior is a very important aspect to take into account on PEM electrolyzer model development but a relatively low number of papers include dynamic responses to voltage perturbations. Also, the description of two-phase flow effects (water and gas dynamics in the channels) is rare in CFD models used to simulate the PEM electrolyzer performance, mainly due to the corresponding extremely high simulation times. However, the inclusion of two-phase flow effects on PEM electrolyzer's model simulation is very important to simulate accurately its performance as well as to be possible to suggest new bipolar plates configurations as well as the most suitable materials to PTLs. Other issue that should be included in PEM electrolyzer models development is the performance degradation due to components ageing. So far there are no studies on this subject, crucial to develop PEM electrolyzers with a higher durability and, consequently, with a lower cost considering its useful lifetime, which will certainly increase the TRL.

This review aims to be useful for the beginners on PEM electrolyzer modeling area, providing a compilation of the models published in the last years, including the equations used to model cell voltage and enlightening important aspects that should be taken into account on PEM electrolyzer models further development.

Table 2
Software used to implement the developed models found in literature.

Reference	Software/algorithms used
Harrison et al. (2005)	Mathematica
Görgün (2006)	MATLAB/Simulink
Biaku et al. (2008)	Mathematica
Dale et al. (2008)	Mathematica
Nie et al. (2008)	ANSYS Fluent
Santarelli et al. (2009)	Yate's method and ANOVA
Awasthi et al. (2011)	MATLAB/Simulink
Agbli et al. (2011)	MATLAB/Simulink
Kim et al. (2013)	MATLAB
Abdol Rahim, Tijani et al. (2015)	MATLAB
Becker and Karri (2010)	MATLAB/Simulink
Oliveira et al. (2013)	MATLAB/Simulink and MEMEPhys
Briguglio et al. (2013)	COMSOL Multiphysics
Abdin et al. (2015)	MATLAB/Simulink
Saeed and Warkozek (2015)	MATLAB
Mohamed et al. (2016)	MATLAB
Yigit and Selamet (2016)	MATLAB/Simulink
Arbabi et al. (2016)	OpenFOAM
Han et al. (2016)	Fortran 90
Aouali et al. (2017)	MATLAB/Simulink
Kaya and Demir (2017)	COMSOL Multiphysics
Sartory et al. (2017)	MATLAB/Simulink
Lee et al. (2019)	OpenPNM

Acknowledgements

This work is a result of the project "UniRCell", with the reference POCI-01-0145-FEDER- 016422 supported by Norte Portugal Regional Operational Programme (NORTE 2020), under the Portugal 2020 Partnership Agreement, through the European Regional Development Fund (FEDER) and by Fundação para a Ciência e Tecnologia (FCT) and also supported by the Project "HYLANTIC"—EAPA_204/2016, which is co-financed by the European Regional Development Found in the framework of the Interreg Atlantic programme.

POCI (FEDER) also supported this work via CEFT, project UID/EMS/00532/2019.

References

Abdin, Z., Webb, C.J., Gray, E.M., 2015. Modelling and simulation of a proton exchange membrane (PEM) electrolyser cell. Int. J. Hydrogen Energy 40, 13243–13257. https://doi.org/10.1016/j.ijhydene.2015.07.129.

Abdol Rahim, A.H., Tijani, A., Farah, T., Shukri, H., 2015. Simulation Analysis of the

Effect of Temperature on Overpotentials in PEM Electrolyzer System.
Agbli, K.S., Péra, M.C., Hissel, D., Rallières, O., Turpin, C., Doumbia, I., 2011. Multi-physics simulation of a PEM electrolyser: energetic macroscopic representation approach. Int. J. Hydrogen Energy 36, 1382–1398. https://doi.org/10.1016/j.ijhydene.2010.10.069.
Aouali, F.Z., Becherif, M., Ramadan, H.S., Emziane, M., Khellaf, A., Mohammedi, K., 2017. Analytical modelling and experimental validation of proton exchange membrane electrolyser for hydrogen production. Int. J. Hydrogen Energy 42, 1366–1374. https://doi.org/10.1016/j.ijhydene.2016.03.101.
Aouali, F.Z., Becherif, M., Tabanjat, A., Emziane, M., Mohammedi, K., Krehi, S., Khellaf, A., 2014. Modelling and experimental analysis of a PEM electrolyser powered by a solar photovoltaic panel. Energy Procedia 62, 714–722. https://doi.org/10.1016/j.egypro.2014.12.435.
Arbabi, F., Montazeri, H., Abouatallah, R., Wang, R., Bazylak, A., 2016. Three-dimensional computational fluid dynamics modelling of oxygen bubble transport in polymer electrolyte membrane electrolyzer porous transport layers. J. Electrochem. Soc. 163, F3062–F3069. https://doi.org/10.1149/2.0091611jes.
Atlam, O., Kolhe, M., 2011. Equivalent electrical model for a proton exchange membrane (PEM) electrolyser. Energy Convers. Manag. 52, 2952–2957. https://doi.org/10.1016/j.enconman.2011.04.007.
Awasthi, A., Scott, K., Basu, S., 2011. Dynamic modeling and simulation of a proton exchange membrane electrolyzer for hydrogen production. Int. J. Hydrogen Energy 36, 14779–14786. https://doi.org/10.1016/j.ijhydene.2011.03.045.
Barbir, F., 2005. PEM electrolysis for production of hydrogen from renewable energy sources. Sol. Energy 78, 661–669. https://doi.org/10.1016/j.solener.2004.09.003.
Becker, S., Karri, V., 2010. Predictive models for PEM-electrolyzer performance using adaptive neuro-fuzzy inference systems. Int. J. Hydrogen Energy 35, 9963–9972. https://doi.org/10.1016/j.ijhydene.2009.11.060.
Bessarabov, D., wang, H., Li, H., Zhao, N., 2015. PEM Electrolysis for Hydrogen Production: Principles and Applications.
Biaku, C.Y., Dale, N.V., Mann, M.D., Salehfar, H., Peters, A.J., Han, T., 2008. A semiempirical study of the temperature dependence of the anode charge transfer coefficient of a 6 kW PEM electrolyzer. Int. J. Hydrogen Energy 33, 4247–4254. https://doi.org/10.1016/j.ijhydene.2008.06.006.
Briguglio, N., Brunaccini, G., Siracusano, S., Randazzo, N., Dispenza, G., Ferraro, M., Ornelas, R., Aricò, A.S., Antonucci, V., 2013. Design and testing of a compact PEM electrolyzer system. Int. J. Hydrogen Energy 38, 11519–11529. https://doi.org/10.1016/j.ijhydene.2013.04.091.
Brown, T.M., Brouwer, J., Samuelsen, G.S., Holcomb, F.H., King, J., 2008. Dynamic first principles model of a complete reversible fuel cell system. J. Power Sources 182, 240–253. https://doi.org/10.1016/j.jpowsour.2008.03.077.
Carmo, M., Fritz, D.L., Mergel, J., Stolten, D., 2013. A comprehensive review on PEM water electrolysis. Int. J. Hydrogen Energy 38, 4901–4934. https://doi.org/10.1016/j.ijhydene.2013.01.151.
Chandesris, M., Médeau, V., Guillet, N., Chelghoum, S., Thoby, D., Fouda-Onana, F., 2015. Membrane degradation in PEM water electrolyzer: numerical modeling and experimental evidence of the influence of temperature and current density. Int. J. Hydrogen Energy 40, 1353–1366. https://doi.org/10.1016/j.ijhydene.2014.11.111.
Choi, P., Bessarabov, D.G., Datta, R., 2004. A simple model for solid polymer electrolyte (SPE) water electrolysis. Solid State Ionics 175, 535–539. https://doi.org/10.1016/j.ssi.2004.01.076.
Dale, N.V., Mann, M.D., Salehfar, H., 2008. Semiempirical model based on thermodynamic principles for determining 6 kW proton exchange membrane electrolyzer stack characteristics. J. Power Sources 185, 1348–1353. https://doi.org/10.1016/j.jpowsour.2008.08.054.
García-Valverde, R., Espinosa, N., Urbina, A., 2012. Simple PEM water electrolyser model and experimental validation. Int. J. Hydrogen Energy 37, 1927–1938. https://doi.org/10.1016/j.ijhydene.2011.09.027.
Görgün, H., 2006. Dynamic modelling of a proton exchange membrane (PEM) electrolyzer. Int. J. Hydrogen Energy 31, 29–38. https://doi.org/10.1016/j.ijhydene.2005.04.001.
Han, B., Mo, J., Kang, Z., Zhang, F.-Y., 2016. Effects of membrane electrode assembly properties on two-phase transport and performance in proton exchange membrane electrolyzer cells. Electrochim. Acta 188, 317–326. https://doi.org/10.1016/j.electacta.2015.11.139.
Harrison, K.W., Hernández-Pacheco, E., Mann, M., Salehfar, H., 2005. Semiempirical model for determining PEM electrolyzer stack characteristics. J. Fuel Cell Sci. Technol. 3, 220–223. https://doi.org/10.1115/1.2174072.
Hwang, J.J., Lai, L.K., Wu, W., Chang, W.R., 2009. Dynamic modeling of a photovoltaic hydrogen fuel cell hybrid system. Int. J. Hydrogen Energy 34, 9531–9542. https://doi.org/10.1016/j.ijhydene.2009.09.100.
Kaya, M.F., Demir, N., 2017. Numerical investigation of PEM water electrolysis performance for different oxygen evolution electrocatalysts. Fuel Cell. 17, 37–47. https://doi.org/10.1002/fuce.201600216.
Kim, H., Park, M., Lee, K.S., 2013. One-dimensional dynamic modeling of a high-pressure water electrolysis system for hydrogen production. Int. J. Hydrogen Energy 38, 2596–2609. https://doi.org/10.1016/j.ijhydene.2012.12.006.
Lamy, C., 2016. From hydrogen production by water electrolysis to its utilization in a PEM fuel cell or in a SO fuel cell: some considerations on the energy efficiencies. Int. J. Hydrogen Energy 41, 15415–15425. https://doi.org/10.1016/j.ijhydene.2016.04.173.
Lebbal, M.E., Lecœuche, S., 2009. Identification and monitoring of a PEM electrolyser based on dynamical modelling. Int. J. Hydrogen Energy 34, 5992–5999. https://doi.org/10.1016/j.ijhydene.2009.02.003.
Lee, J.K., Lee, C.H., Bazylak, A., 2019. Pore network modelling to enhance liquid water transport through porous transport layers for polymer electrolyte membrane electrolyzers. J. Power Sources 10, 1016/j.jpowsour.2019.226910.
Marangio, F., Santarelli, M., Calì, M., 2009. Theoretical model and experimental analysis of a high pressure PEM water electrolyser for hydrogen production. Int. J. Hydrogen Energy 34, 1143–1158. https://doi.org/10.1016/j.ijhydene.2008.11.083.
Medina, P., Santarelli, M., 2010. Analysis of water transport in a high pressure PEM electrolyzer. Int. J. Hydrogen Energy 35, 5173–5186. https://doi.org/10.1016/j.ijhydene.2010.02.130.
Mohamed, B., Alli, B., Ahmed, B., 2016. Using the hydrogen for sustainable energy storage: designs, modeling, identification and simulation membrane behavior in PEM system electrolyser. J. Energy Storage 7, 270–285. https://doi.org/10.1016/j.est.2016.06.006.
Moradi Nafchi, F., Afshari, E., Baniasadi, E., Javani, N., 2019. A parametric study of polymer membrane electrolyser performance, energy and exergy analyses. Int. J. Hydrogen Energy 44, 18662–18670. https://doi.org/10.1016/j.ijhydene.2018.11.081.
Myles, T.D., Nelson, G.J., Peracchio, A.A., Roy, R.J., Murach, B.L., Adamson, G.A., Chiu, W.K.S., 2012. Species transport in a high-pressure oxygen-generating proton-exchange membrane electrolyzer. Int. J. Hydrogen Energy 37, 12451–12463. https://doi.org/10.1016/j.ijhydene.2012.05.123.
Nafeh, A.E.-S.A., 2011. Hydrogen production from a PV/PEM electrolyzer system using a neural-network-based MPPT algorithm. Int. J. Numer. Model. Electron. Network. Dev. Field. 24, 282–297. https://doi.org/10.1002/jnm.778.
Ni, M., Leung, M.K.H., Leung, D.Y.C., 2008. Energy and exergy analysis of hydrogen production by a proton exchange membrane (PEM) electrolyzer plant. Energy Convers. Manag. 49, 2748–2756. https://doi.org/10.1016/j.enconman.2008.03.018.
Nie, J., Chen, Y., 2010. Numerical modeling of three-dimensional two-phase gas–liquid flow in the flow field plate of a PEM electrolysis cell. Int. J. Hydrogen Energy 35, 3183–3197. https://doi.org/10.1016/j.ijhydene.2010.01.050.
Nie, J., Chen, Y., Boehm, R.F., 2008. Numerical Modeling of Two-phase Flow in a Bipolar Plate of a PEM Electrolyzer Cell, pp. 783–788. https://doi.org/10.1115/IMECE2008-68913.
Nie, J., Chen, Y., Cohen, S., Carter, B.D., Boehm, R.F., 2009. Numerical and experimental study of three-dimensional fluid flow in the bipolar plate of a PEM electrolysis cell. Int. J. Therm. Sci. 48, 1914–1922. https://doi.org/10.1016/j.ijthermalsci.2009.02.017.
Oliveira, L.F.L., Jallut, C., Franco, A.A., 2013. A multiscale physical model of a polymer electrolyte membrane water electrolyzer. Electrochim. Acta 110, 363–374. https://doi.org/10.1016/j.electacta.2013.07.214.
Olivier, P., Bourasseau, C., Bouamama, P.B., 2017. Low-temperature electrolysis system modelling: a review. Renew. Sustain. Energy Rev. 78, 280–300. https://doi.org/10.1016/j.rser.2017.03.099.
Onda, K., Murakami, T., Hikosaka, T., Kobayashi, M., Notu, R., Ito, K., 2002. Performance analysis of polymer-electrolyte water electrolysis cell at a small-unit test cell and performance prediction of large stacked cell. J. Electrochem. Soc. 149, A1069–A1078. https://doi.org/10.1149/1.1492287.
Ruuskanen, V., Koponen, J., Huoman, K., Kosonen, A., Niemelä, M., Ahola, J., 2017. PEM water electrolyzer model for a power-hardware-in-loop simulator. Int. J. Hydrogen Energy 42, 10775–10784. https://doi.org/10.1016/j.ijhydene.2017.03.046.
Saeed, E.W., Warkozek, E.G., 2015. Modeling and analysis of renewable PEM fuel cell system. Energy Procedia 74, 87–101. https://doi.org/10.1016/j.egypro.2015.07.527.
Santarelli, M., Medina, P., Calì, M., 2009. Fitting regression model and experimental validation for a high-pressure PEM electrolyzer. Int. J. Hydrogen Energy 34, 2519–2530. https://doi.org/10.1016/j.ijhydene.2008.11.036.
Sartory, M., Wallnöfer-Ogris, E., Salman, P., Fellinger, T., Justl, M., Trattner, A., Klell, M., 2017. Theoretical and experimental analysis of an asymmetric high pressure PEM water electrolyser up to 155 bar. Int. J. Hydrogen Energy 42, 30493–30508. https://doi.org/10.1016/j.ijhydene.2017.10.112.
Sossan, F., Bindner, H., Madsen, H., Torregrossa, D., Chamorro, L.R., Paolone, M., 2014. A model predictive control strategy for the space heating of a smart building including cogeneration of a fuel cell-electrolyzer system. Int. J. Electr. Power Energy Syst. 62, 879–889. https://doi.org/10.1016/j.ijepes.2014.05.040.
Tijani, A.S., Binti Kamarudin, N.A., Binti Mazlan, F.A., 2018. Investigation of the effect of charge transfer coefficient (CTC) on the operating voltage of polymer electrolyte membrane (PEM) electrolyzer. Int. J. Hydrogen Energy 43, 9119–9132. https://doi.org/10.1016/j.ijhydene.2018.03.111.
Toghyani, S., Afshari, E., Baniasadi, E., 2018. Three-dimensional computational fluid dynamics modeling of proton exchange membrane electrolyzer with new flow field pattern. J. Therm. Anal. Calorim. 10, 1007/s10973-018-7236-5.
Toghyani, S., Fakhradini, S., Afshari, E., Baniasadi, E., Abdollahzadeh Jamalabadi, M.Y., Safdari Shadloo, M., 2019. Optimization of operating parameters of a polymer exchange membrane electrolyzer. Int. J. Hydrogen Energy 44, 6403–6414. https://doi.org/10.1016/j.ijhydene.2019.01.186.
Touré, S., Konaté, A., Traoré, D., Fofana, D., 2018. Novel determination method of charge transfer coefficient of PEM fuel cell using the Lagrange's multiplier method. IOP Conf. Ser. Earth Environ. Sci. 188 https://doi.org/10.1088/1755-1315/188/1/012041, 012041.
Yigit, T., Selamet, O.F., 2016. Mathematical modeling and dynamic Simulink simulation of high-pressure PEM electrolyzer system. Int. J. Hydrogen Energy 41, 13901–13914. https://doi.org/10.1016/j.ijhydene.2016.06.022.